ADVANCED FUNCTIONAL MATERIALS
www.afm-journal.de

Stable White Afterglow Along the Blackbody Radiation Line Enabled by Assisted Partial Phosphorescence Resonance Energy Transfer

*Tongyue Wu, Peilong Liao, Weilin Qi, Huaiyu Song, Hongpeng Li, Jianbin Huang, and Yun Yan**

White afterglow is very appealing both in scenario-specific luminescence and background-free bio-imaging, while it is challenging to obtain stable white afterglow due to the difficulty in matching the emission lifetimes of complementary colors. It is reported here that assisted partial phosphorescence resonance energy transfer (ap-PRET) can be a very efficient way toward this goal. When a blue afterglow of energy donor with long lifetime is obtained in a polymeric network displaying phosphorescent clusterization-triggered emission (CTE), the network assisted partial phosphorescence resonance energy transfer (ap-PRET) between it and a yellow fluorescent acceptor would yields orange afterglow. Owing to the energy supply of the CTE network, the lifetime of the donors blue afterglow can be tuned close to that of the acceptors orange afterglow through ap-PRET in a wide donor to accepter ratios, and emissions ranging from the cold to warm white afterglows can be obtained. Amazingly, these white afterglows are along the blackbody radiation line in the CIE plot, disclosing the powerful ability of ap-PRET in generating desired white afterglows for applications in diversified luminescent scenarios.

1. Introduction

White afterglows are becoming increasingly important in background-independent bio-emitting and night-vision surveillance.[1] Currently, white afterglow is mainly achieved through combinations of complementary emissions of blue and yellow[2] or red, green and blue[3] from different materials. Except these efforts, single molecular white phosphorescence materials have also been reported.[4a,b] However, due to the difficulty in balancing both the emission intensity and lifetime of different colors at the same time, white afterglow is usually observed at a glimpse.[5] So far few stable white afterglow materials have been reported.[3,6]

Theoretically, white emission not merely refers to a single point shown in chromatic coordinates. In terms of color temperatures, white emission may expand the large panel from 2000 to 10 000 K. For example, the color temperature of warm white light from high-pressure sodium lamp is ≈2000–2100 K, that of incandescent lamp is 2800 K, while the cold white light from fluorescent lamp is 6500 K. All these white afterglows can be gathered into a special curved line in the CIE plot, which is called Plank blackbody radiation line.[7] In practical applications, it is difficult to obtain all the white emissions along the blackbody radiation line through direct combination of complementary colors since the blackbody radiation line is not straight.[8a,b] For this reason, people often merely obtain a single white emission corresponding to one color temperature through complementary colors.[9a,b] Up to date, it is still unknown how to obtain the broad spectrum of white emissions along the blackbody radiation line through color combination.[10]

Recently, phosphorescence resonance energy transfer (PRET) is reported to occur between phosphorescent donors and acceptor dyes,[11a,b] just like the fluorescent resonance energy transfer (FRET) between fluorescent donors and acceptors.[12a,b] Interestingly, the acceptor dyes in PRET are not necessarily phosphorescent molecules; instead, they can simply be fluorescent ones.[13a,b] The well-known evidence for the occurrence of PRET is the gradually decreased donor lifetime and the increased acceptor lifetime from ns to ms.[14] Both the lifetimes of the donor and acceptor can be fine-tuned by varying the molar ratio between them.[15] At proper molar ratios, their lifetimes are comparable and both the emissions of the donor and acceptor exist.[16a,b] This inspires that if a partial PRET process is rationally designed, one may obtain stable white afterglow in a broad donor to acceptor ratios. However, previous studies focus a lot on the complete resonance energy transfer process,[17a,b] and few

T. Wu, P. Liao, W. Qi, H. Song, H. Li, J. Huang, Y. Yan
Beijing National Laboratory for Molecular Sciences (BNLMS)
College of Chemistry and Molecular Engineering
Peking University
Beijing 100871, P. R. China
E-mail: yunyan@pku.edu.cn

Y. Yan
Ningxia Key Laboratory of Green Catalytic Materials and Technology
College of Chemistry and Chemical Engineering
Ningxia Normal University
Guyuan 756000, P. R. China

The ORCID identification number(s) for the author(s) of this article can be found under https://doi.org/10.1002/adfm.202415525

DOI: 10.1002/adfm.202415525

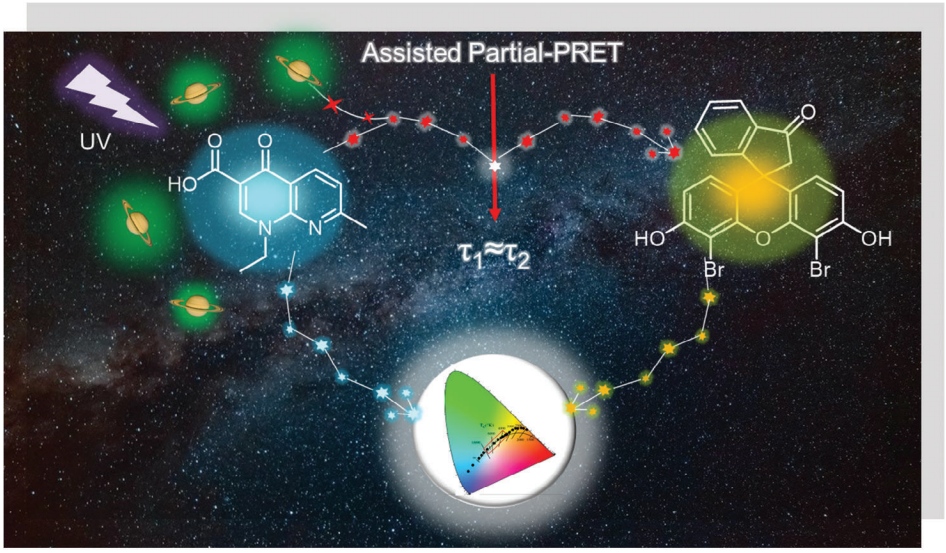

Scheme 1. Construction of white afterglow through assisted partial phosphorescence energy transfer.

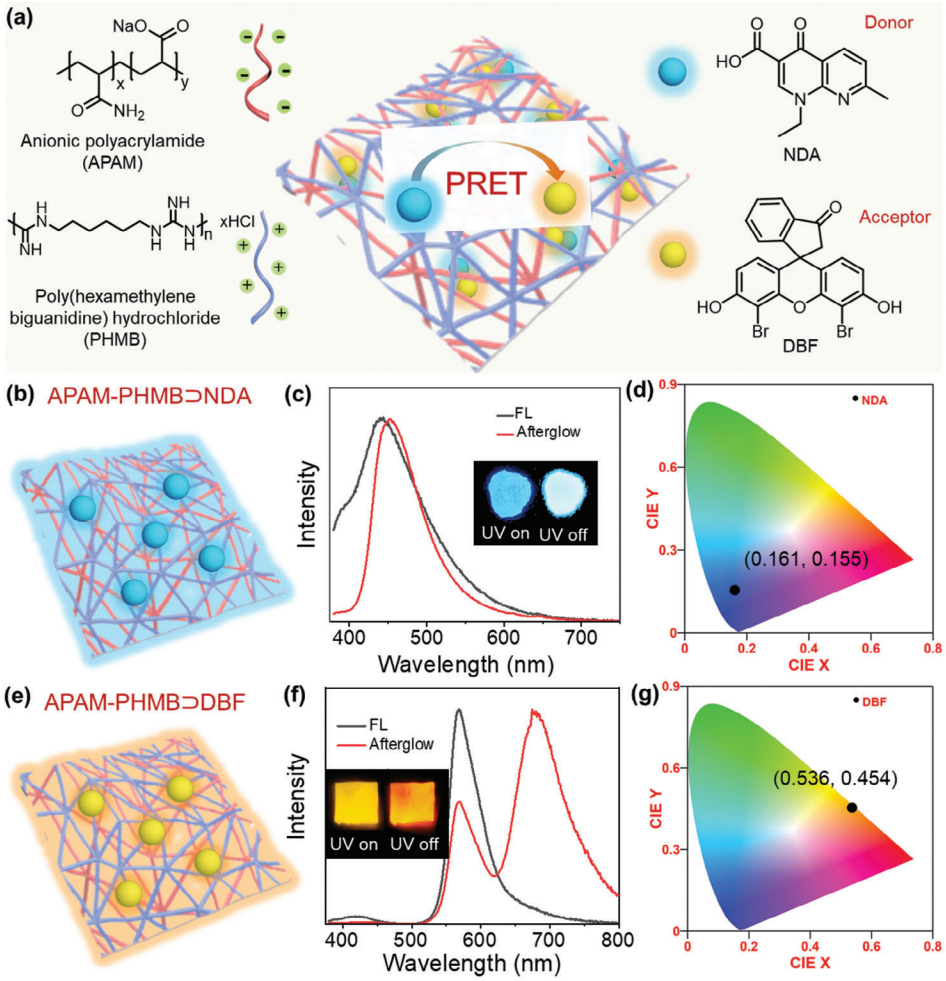

Figure 1. a, b and e) The schematic illustration of the (a) APAM-PHMB⊃NDA+DBF partial PRET(p-PRET) system, (b) APAM-PHMB⊃NDA flake and (e) APAM-PHMB⊃DBF flake. c and f) Fluorescence and afterglow emission spectra of (c) NDA and (f) DBF. d and g) CIE chromaticity diagram of the afterglow of (d) NDA and (g) DBF.

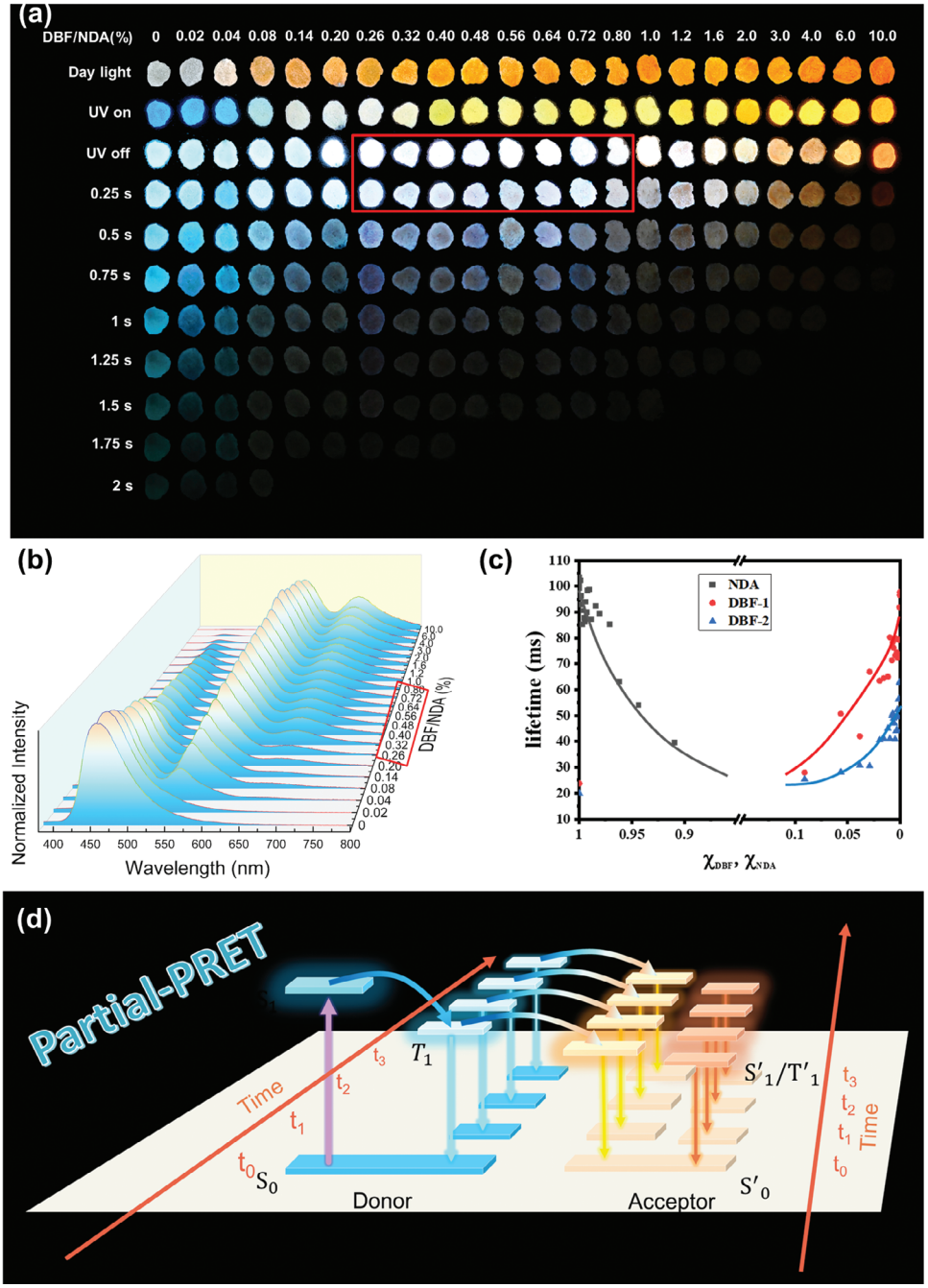

Figure 2. a) Photos of APAM-PHMB⊃NDA+DBF flake with different DBF / NDA ratios (under ambient light), fluorescence photos (Ex = 365 nm) and long afterglow photos (Ex = 365 nm) with different delay times. b) Long afterglow spectra (Ex = 365 nm) of APAM-PHMB⊃NDA+DBF flake with different DBF / NDA ratios. c) Long afterglow lifetime of APAM-PHMB⊃NDA+DBF flakes with different DBF / NDA molar ratios under Ex = 365 nm. (X_{DBF} = $n_{DBF}/(n_{DBF}+n_{NDA})$ d) Schematic illustration of the mechanism of partial PRET between NDA and DBF.

attention has been made to obtain white emissions with partial PRET.

Herein, we report the generation of a wide spectrum of white afterglows along the blackbody radiation line through polymeric network assisted partial PRET (ap-PRET). We show that upon achieving blue afterglows by restricting the fluorescent dye in a densely woven polymeric network, introducing a yellow fluorescent dye allows the occurrence of PRET between them. Owing to the contribution of phosphorescent clusterization triggered emission (CTE) of the polymeric network, the lifetime of the donor does not decrease drastically with increasing the fraction of acceptor. As a result, there exists a broad window of donor/acceptor ratios where their emission lifetimes are comparably long. Consequently, a series of afterglows ranging from

Table 1. Long afterglow lifetime of APAM-PHMB⊃NDA+DBF with different DBF / NDA ratios under the excitation of 365 and 450 nm.

DBF/NDA [%]	Ex = 365 nm						Ex = 450 nm			
	NDA		DBF-1		DBF-2		DBF-1		DBF-2	
	Wavelength [nm]	Lifetime [ms]	Wavelength [nm]	Lifetime [ms]	Wavelength [nm]	Lifetime [ms]	Wavelength [nm]	Lifetime [ms]	Wavelength [nm]	Lifetime [ms]
0	457	103.48								
0.02	454	100.35	542	97.78						
0.04	453	99.25	547	96.64						
0.08	451	95.52	553	91.94	672	62.86	553	33.2	672	30.08
0.14	447	102.19	555	79.33	668	56.41				
0.20	448	96.27	554	72.74	667	49.49	554	31.96	667	30.51
0.26	**447**	**92.81**	**557**	**72.48**	**668**	**52.29**				
0.32	**448**	**85.24**	**561**	**74.43**	**674**	**44.53**				
0.40	**448**	**90.53**	**563**	**79.83**	**675**	**44.02**	**563**	**32.77**	**675**	**29.18**
0.48	**443**	**87.73**	**566**	**73.27**	**675**	**40.79**				
0.56	**443**	**86.27**	**565**	**79.86**	**673**	**47**				
0.64	**443**	**83.94**	**565**	**76.24**	**673**	**49.04**				
0.72	**443**	**89.96**	**565**	**78.28**	**673**	**50.82**				
0.80	**443**	**98.36**	**566**	**71.36**	**673**	**49.94**	**566**	**32.68**	**673**	**26.8**
1.0	443	98.7	566	80.24	673	41.13				
1.2	443	87.13	565	65.04	673	44.99	565	34.1	673	31.62
1.6	443	92.37	568	64.48	674	41.15	568	33.11	674	28.59
2.0	442	89.42	571	63.5	674	40.54	571	28.31	675	24.71
3.0	440	95.31	574	66.96	677	30.5	574	24.85	677	23.22
4.0	440	63.05	577	42.05	679	30.73	577	26.12	679	21.58
6.0	440	54.13	579	50.72	681	28.19	579	22.41	681	21.8
10.0	440	39.55	584	28.02	684	25.4	584	20.68	684	17.61

[a] 450 nm light is able to directly excite DBF; [b] The bold results (DBF/NDA = 0.26–0.80%) represent the data related to the white afterglow flakes.

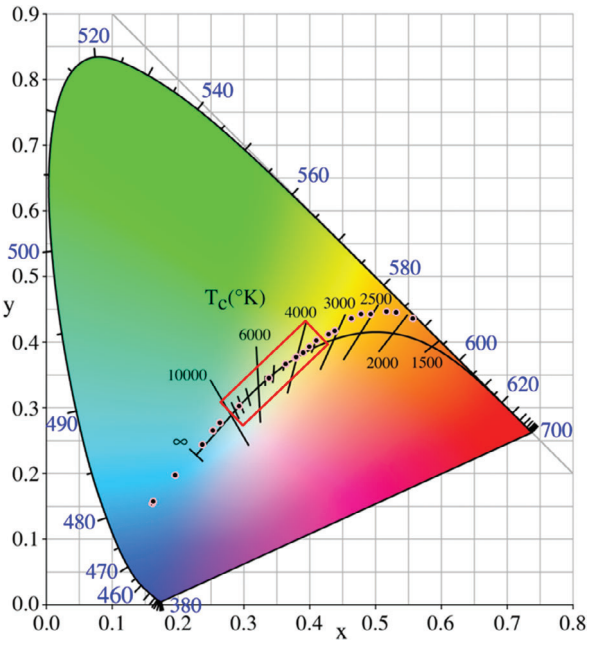

Figure 3. CIE chromatogram of APAM-PHMB⊃NDA+DBF flakes with different DBF/NDA molar ratio (Ex = 365 nm).

cold to warm white light along the curved blackbody radiation line were obtained, which is very promising in achieving desired white light for specific applications (**Scheme 1**).

Figure 1a is the schematic demonstration of the construction of the ap-PRET system. As reported in our earlier work, the electrostatic network of oppositely charged polymers are able to endow all the doped fluorescent molecules with emissions of long lifetime, including phosphorescence or delayed fluorescence[18] through CTE phosphorescence resonance energy transfer. The polymeric network formed with the anionic polyacrylamide (APAM) and the cationic polyhexamethylene biguanidine hydrochloride (PHMB), denoted as APAM-PHMB, was employed in this work owing to the best performance. The blue fluorescent dye NDA and the yellow fluorescent DBF was selected as the donor and acceptor, respectively, since the emission of NDA overlaps with the absorption of DBF (Figure S1, Supporting Information). Figure 1a shows that NDA in the APAM-PHMB network(APAM-PHMB⊃NDA) exhibits blue fluorescence with the maxima at 445 nm and bright blue phosphorescence with the maxima at 457 under 365 nm illumination. The phosphorescence lifetime ($<\tau>_p$) of NDA is 103 ms (Figure 1c). The CIE coordinate of the phosphorescence of NDA is (0.161, 0.155) (Figure 1d). Similarly, DBF in the APAM-PHMB network (APAM-PHMB⊃DBF) displays orange fluorescence with

Table 2. Color evaluation of APAM-PHMB⊃NDA+DBF flake with different DBF/NDA ratios.

DBF/NDA [%]	CRI	xy_CCT	uv_CCT	Duv	x	y
0	33.4	−613	147 922	0.0715	0.161	0.155
0.02	34.2	−3614	147 916	0.0700	0.162	0.157
0.04	59.6	1 198 343	147 616	0.0358	0.196	0.198
0.08	66.6	28 024	77 824	0.0071	0.237	0.244
0.14	64.3	16 202	18 480	0.0063	0.253	0.265
0.20	62.3	12 660	13 250	0.0047	0.264	0.277
0.26	**58.3**	**8181**	**8204**	**−0.0003**	**0.293**	**0.302**
0.32	**49.4**	**5215**	**5212**	**−0.0010**	**0.339**	**0.345**
0.40	**46.5**	**4402**	**4396**	**−0.0001**	**0.364**	**0.366**
0.48	**43.6**	**4051**	**4042**	**0.0000**	**0.379**	**0.376**
0.56	**42.7**	**4004**	**3995**	**0.0000**	**0.381**	**0.377**
0.64	**41.4**	**3785**	**3775**	**0.0002**	**0.391**	**0.383**
0.72	**40.3**	**3644**	**3636**	**0.0024**	**0.400**	**0.394**
0.80	**39.3**	**3489**	**3483**	**0.0040**	**0.411**	**0.403**
1.0	37.1	3194	3189	0.0044	0.430	0.412
1.2	35.4	3082	3077	0.0052	0.439	0.418
1.6	30.6	2840	2838	0.0087	0.463	0.436
2.0	30.2	2699	2697	0.0100	0.478	0.443
3.0	28.5	2517	2517	0.0089	0.493	0.442
4.0	27.0	2294	2295	0.0096	0.517	0.447
6.0	25.7	2155	2156	0.0095	0.532	0.446
10.0	24.8	1908	1901	0.0079	0.557	0.436

[a] CRI: color rendering index; [b] CCT: color temperature, that means the temperature of blackbody radiation is uesd to represent the corresponding color; [c] xy_CCT: The color temperature based on the 1931 standard CIE (x, y) chromaticity diagram is represented as xy_CCT; [d] uv_CCT: The color temperature based on the 1976 standard CIE (u, v) chromaticity diagram is represented as uv_CCT; [e] Duv: Color deviation. The minimum distance between the color of the light source and the blackbody radiation curve. The smaller the color deviation, the closer the light source is to the corresponding blackbody radiation color; [f] The bold results (DBF/NDA = 0.26–0.80%) represents the data related to the white afterglow flakes.

the maxima at 567 nm. After cessation of irradiation, an orange-red afterglow composed of delayed fluorescence at 567 nm and phosphorescence at 675 nm can be detected. The delayed fluorescence lifetime ($<\tau>_{DF}$) and the phosphorescence lifetime ($<\tau>$p) are 23.8 and 20 ms, respectively (Figure 1f). The CIE coordinate of the afterglow of DBF is (0.536, 0.454) (Figure 1g). Clearly, although the colors of the two materials are complementary to each other, their lifetimes are drastically different, making it difficult to obtain stable white afterglow.

Next, both NDA and DBF were doped into the APAM-PHMB matrix. **Figure** 2a shows that with increasing the molar fraction of DBF, the color of the flake turns gradually from white to dark orange red. The normalized three-dimensional concentration-long afterglow spectra in Figure 2b demonstrate that with increase of the DBF / NDA molar ratio, the peak intensity of the donor NDA ≈440–460 nm decreased gradually, while the delayed fluorescence peak (DBF-1, 540–580 nm) and phosphorescence peak (DBF-2, 670–685 nm) belonging to the acceptor DBF increased, showing an obvious PRET process. As the DBF / NDA molar ratio is beyond 3%, the emission peak of NDA disappeared completely, while the delayed fluorescence peak (540-580 nm) of DBF remained unchanged. Meanwhile, the phosphorescence peak (670–685 nm) of DBF was further enhanced.

Since we aim to obtain white afterglows, the emission lifetimes under different partial PRET conditions were further investigated. As revealed in Figure 2c and **Table 1**, as DBF / NDA ratio is in the range of 0.26–0.80%, the lifetime of NDA remains nearly constant at ≈90 ms with increasing DBF, while the emission lifetimes for DBF-1 have been significantly promoted from 23 to over 70 ms, and those of DBF-2 from 20 to over 40 ms. This means that the energy received by DBF is not merely from NDA. Indeed, the APAM-PHMB matrix also serves as the energy donor for DBF with its clustrization-triggered emission (CTE).[18] Upon excitation with 365 nm UV light, APAM-PHMB matrix display green CTE phosphorescence at room temperature, which is a broad band centered at 500 nm.[18] Since the energy for the T_1^* state of CTE is closer to the S_1^* state of DBF than the T_1^* of NDA, DBF receives energy from CTE easier than from NDA. As a result, the lifetime of NDA is not affected noticeably with increasing DBF/NDA ratio. It is noticed the apparent energy transfer efficiencies between NDA and DBF is in the range of 5–20%(Figure S2, Supporting Information).With this unique polymeric network assisted partial PRET (ap-PRET) mechanism, both the donor emission and acceptor emission are obtained in a broad window of DBF/NDA ratio, and stable white afterglows were obtained in the range of 0.26–0.80%. In addition, the white afterglows are also stable in the broad temperature window of 77K–350K and relative humidity (RH) range of 0–57% (Tables S1 and S2; Figures S3 and S4, Supporting Information). It is worth noting that the lifetimes of DBF obtained from ap-PRET are drastically larger than those through direct excitation with 450 nm (Table 1), manifesting the ap-PRET process is advantageous in boosting the emission lifetime of the acceptor DBF.

The ap-PRET enabled wide range of stable phosphorescence lifetime of NDA and DBF in the APAM-PMHB matrix allows fine tune the CIE coordinates of the white afterglows. Using color algorithm data package (shown in SI), the spectrum can be converted into corresponding CIE (x, y) coordinates. Excitingly, the CIE coordinates of the white afterglows were found to gather on the curved Planck blackbody radiation line(**Figure 3** and **Table 2**). This means that all the white afterglows obtained in this work are standard white emissions corresponding to different color temperatures. Detailed study reveals that the CCT (Correlated Color Temperature) of these white lights covers the range from reddish 3400 K to bluish over 8000 K, and the color deviation Duv is less than 0.01. In particular, when the DBF / NDA molar ratio is 0.26%, the CIE coordinates are (0.293, 0.302), showing a cold white light of 8204 K. When the ratio of DBF / NDA is 0.32%, the coordinates are (0.339, 0.345) and it shows positive white light at 5212 K. As the DBF / NDA ratio is 0.40% – 0.80%, the coordinates increase from (0.364, 0.366) to (0.411, 0.403), showing a warm white light of 4396–3483 K. In current market, the white light sources, especially white LED (WLED) devices, have a CCT of above 6000 K and the light color is bluish, which is benefit for outdoor lighting.[19a,b] However, as for indoor lighting, warm white light with a reddish color and a CCT ≈3000 K is strongly desired to avoid the human eyes from staving off.[20] Thus, the wide CCT regulating ability of APAM-PHMB⊃NDA+DBF flakes

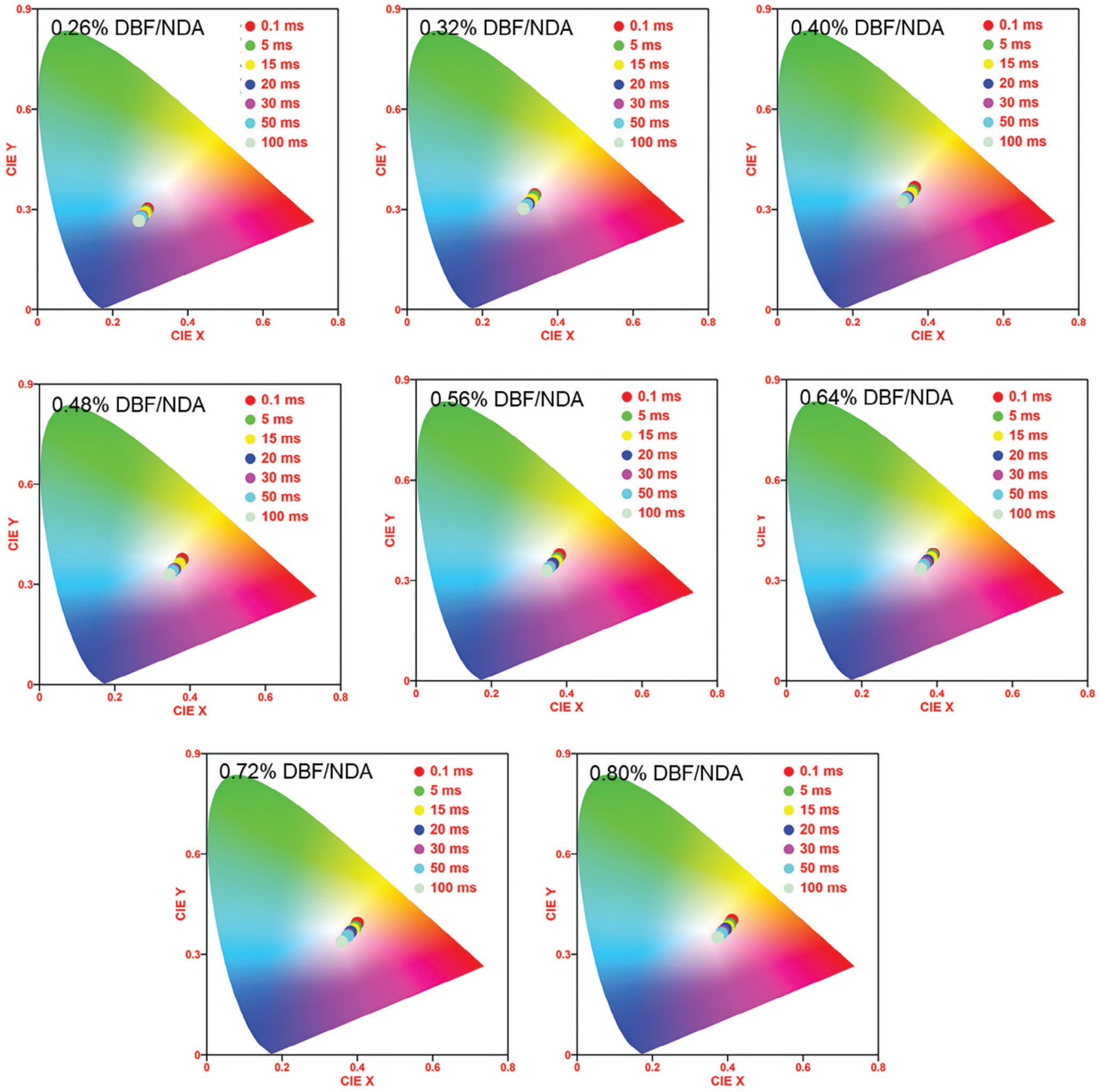

Figure 4. Time stability of the white afterglow of APAM-PHMB⊃NDA+DBF flake with DBF/NDA ranging 0.26%–0.8%.

made it a good candidate for white light sources in the next generation of lighting applications.[21]

2. Time Stability of the White Afterglow

Finally, the time stability of the white afterglow is evaluated. As shown in **Figure 4** and **Table 3**, the color of the long afterglow slightly blue shifts with prolonging the delay time. This is because the lifetimes of the long wave acceptor emission of DBF-1 and DBF-2 is shorter than that of the donor emissions with shorter wavelength. Although the change of luminescent color is inevitable with decay time, the absolute deviation of the CIE coordinates within 15 ms is very small, which is smaller than 0.01 for $\Delta x_{15\ ms}$ ($\Delta x_{15\ ms} < 0.01$), and in between 0.01 and 0.02 for $\Delta y_{15\ ms}$ ($0.01 < \Delta y_{15\ ms} < 0.02$). In line with the small CIE coordinates deviation, the correlated color temperature deviation $\Delta CCT_{15\ ms}/CCT$ is less than 8%, which reflects that the white light stability is rather small in this given time range. Compared with the white phosphorescence only stable for a glimpse,[5,22a,b] it can be considered that the white phosphorescence originated from APAM-PHMB⊃NDA+DBF has a fairly good stability.

Table 3. The stability of white afterglow of APAM-PHMB⊃NDA+DBF flake in 0.26% – 0.8% DBF/NDA ratio.

DBF/NDA [%]	CCT	$CCT_{15\ ms}$	$\Delta CCT_{15\ ms}$/CCT [%]	$\Delta x_{15\ ms}$	$\Delta y_{15\ ms}$	$CCT_{100\ ms}$	$\Delta CCT_{100\ ms}$/CCT [%]	$\Delta x_{100\ ms}$	$\Delta y_{100\ ms}$
0.26	8204	8827	7.594	−0.007	−0.011	12 770	55.66	−0.022	−0.031
0.32	5212	5548	6.447	−0.008	−0.014	6949	33.33	−0.030	−0.043
0.40	4396	4606	4.777	−0.009	−0.017	5512	25.39	−0.033	−0.046
0.48	4042	4136	2.326	−0.007	−0.014	4907	21.40	−0.034	−0.047
0.56	3995	4125	3.254	−0.009	−0.018	4890	22.40	−0.035	−0.048
0.64	3775	3843	1.801	−0.006	−0.011	4459	18.12	−0.033	−0.043
0.72	3636	3732	2.640	−0.010	−0.018	4419	21.53	−0.042	−0.056
0.80	3483	3526	1.235	−0.009	−0.019	4031	15.73	−0.038	−0.050

[a] The CCT is the uv_CCT of APAM-PHMB⊃NDA+DBF calculated by Ohno 2013 method based on the long afterglow spectrum with a delay time of 0.1 ms; [b] The $CCT_{15\ ms}$ and $CCT_{100\ ms}$ is the uv_CCT of APAM-PHMB⊃NDA+DBF with a delay time of 15 and 100 ms calculated by the same method; [c] $\Delta x_{15\ ms}$ and $\Delta y_{15\ ms}$ is the displacement of CIE (x, y) coordinate with delay time from 0.1 ms to 15 ms, while $\Delta x_{100\ ms}$ and $\Delta y_{100\ ms}$ is the displacement of CIE (x, y) coordinate with delay time from 0.1 ms to 100 ms, respectively; [d] $\Delta CCT_{15\ ms}$/CCT(%) represents the relative change of color temperature with delay time from 0.1 ms to 15 ms. The calculation formula is: $\Delta CCT_{15\ ms}$/CCT(%) = ($CCT_{15\ ms}$-CCT)/CCT × 100.

3. Conclusion

In summary, this work proposed the strategy of assisted partial PRET (p-PRET) for synergistically regulating the donor and acceptor emission lifetimes to a comparable level. Upon simply initiating the phosphorescence of the blue emissive donor NDA in a densely woven polymeric network composed of strongly interacted ionic polymer APAM and PHMB, the PRET between NDA and the doped acceptor dye DBF allows generation of orange phosphorescence. The assisted PRET between the phosphorescent CTE of the polymeric network to the DBF allows preserving the lifetime of the NDA donor in a rather high level. As a result, there exists a broad range of donor to acceptor ratio where the complementary blue and orange afterglows have similar lifetimes. This generates a wide spectrum of stable white afterglows ranging from warm to cold white along the black body irradiation line. We expect this work inspires rational design of the full spectrum of white afterglows for diversified application scenarios.

Supporting Information

Supporting Information is available from the Wiley Online Library or from the author.

Acknowledgements

The authors are grateful to National Natural Science Foundation of China (Grant No. 22172004, 22332001), National Postdoctoral Researcher Program (GZC20230052) and the Beijing National Laboratory for Molecular Sciences (BNLMS) for financial support.

Conflict of Interest

The authors declare no conflict of interest.

Data Availability Statement

The data that support the findings of this study are available from the corresponding author upon reasonable request.

Keywords

clusterization-triggered emission, phosphorescence lifetime regulation, phosphorescence resonance energy transfer, white afterglow

Received: August 22, 2024
Revised: September 27, 2024
Published online: November 7, 2024

[1] J. Liu, Z. Ma, Z. Li, Y. Liu, X. Fu, H. Jiang, Z. Ma, X. Jia, *J. Mater. Chem. C* **2021**, *9*, 3257.
[2] S. Hirata, M. Vacha, *Adv. Optical Mater.* **2017**, *5*, 1600996.
[3] S. Kuila, S. Garain, S. Bandi, S. J. George, *Adv. Funct. Mater.* **2020**, *30*, 2003693.
[4] a) J. Jin, P. Xue, L. Zhang, H. Jiang, W. Wang, Q. Yang, Y. Tao, C. Zheng, R. Chen, W. Huang, *Angew. Chem., Int. Ed.* **2021**, *60*, 24984; b) Y. Wang, Q. Sun, L. Yue, J. Ma, S. Yuan, D. Liu, H. Zhang, S. Xue, W. Yang, *Adv. Optical Mater.* **2021**, *9*, 2101075.
[5] Y. Liu, Z. Ma, J. Liu, M. Chen, Z. Ma, X. Jia, *Adv. Optical Mater.* **2020**, *9*, 2001685.
[6] X. Zhang, K. C. Chong, Z. Xie, B. Liu, *Angew. Chem., Int. Ed.* **2023**, *62*, 202310335.
[7] Z. Wang, N. Jiang, M. Liu, R. Zhang, F. Huang, D. Chen, *Small* **2021**, *17*, 2104551.
[8] a) H. Gui, Z. Huang, Z. Yuan, X. Ma, *CCS Chem.* **2022**, *4*, 173; b) S. Sun, J. Wang, L. Ma, X. Ma, H. Tian, *Angew. Chem., Int. Ed.* **2021**, *60*, 18557.
[9] a) K. Jinnai, R. Kabe, C. Adachi, *Adv. Mater.* **2018**, *30*, 1800365; b) C. I. Silva Filho, A. L. Oliveira, S. C. F. Pereira, G. F. de Sá, L. L. da Luz, S. Alves, *Dalton Trans.* **2019**, *48*, 2574.
[10] S. Feng, Y. Ma, S. Wang, S. Gao, Q. Huang, H. Zhen, D. Yan, Q. Ling, Z. Lin, *Angew. Chem., Int. Ed.* **2022**, *61*, 202207104.
[11] a) C. Wang, X. K. Ma, P. Guo, C. Jiang, Y. H. Liu, G. Liu, X. Xu, Y. Liu, *Adv. Sci.* **2021**, *9*, 2103041; b) W. Zhang, S. Chen, S. Ye, P. Sun, Q. Fan, J. Song, P. Zeng, J.-L. Qu, W.-Y. Wong, *ACS Materials Lett.* **2022**, *5*, 116.
[12] a) J. Tang, Y. Tian, Z. Lin, C. Zhang, P. Zhang, R. Zeng, S. Wu, X. Chen, J. Chen, *ACS Appl. Mater. Interfaces* **2022**, *15*, 2237; b) H. Wang, J. Tang, H. Deng, Y. Tian, Z. Lin, J. Cui, J. Chen, *J. Mater. Chem. C* **2023**, *11*, 15945.
[13] a) X.-Y. Dai, M. Huo, Y. Liu, *Nat. Rev. Chem.* **2023**, *7*, 854; b) D. Li, Y. Yang, J. Yang, M. Fang, B. Z. Tang, Z. Li, *Nat. Commun.* **2022**, *13*.

[14] S. Xiong, Y. Xiong, D. Wang, Y. Pan, K. Chen, Z. Zhao, D. Wang, B. Z. Tang, *Adv. Mater.* **2023**, *35*, 2301874.
[15] F. Lin, H. Wang, Y. Cao, R. Yu, G. Liang, H. Huang, Y. Mu, Z. Yang, Z. Chi, *Adv. Mater.* **2022**, *34*, 2108333.
[16] a) Y.-X. Hu, P.-P. Jia, C.-W. Zhang, X.-D. Xu, Y. Niu, X. Zhao, Q. Xu, L. Xu, H.-B. Yang, *Org. Chem. Front.* **2021**, *8*, 5250; b) D. Wang, J. Gong, Y. Xiong, H. Wu, Z. Zhao, D. Wang, B. Z. Tang, *Adv. Funct. Mater.* **2022**, *33*, 2208895.
[17] a) N. Melnychuk, S. Egloff, A. Runser, A. Reisch, A. S. Klymchenko, *Angew. Chem., Int. Ed.* **2020**, *59*, 6811; b) J.-X. Wang, Y. Wang, I. Nadinov, J. Yin, L. Gutiérrez-Arzaluz, G. Healing, O. Alkhazragi, Y. Cheng, J. Jia, N. Alsadun, V. S. Kale, C. H. Kang, T. K. Ng, O. Shekhah, H. N. Alshareef, O. M. Bakr, M. Eddaoudi, B. S. Ooi, O. F. Mohammed, *J. Am. Chem. Soc.* **2022**, *144*, 6813.
[18] P. Liao, T. Wu, C. Ma, J. Huang, Y. Yan, *Adv. Optical Mater.* **2022**, *11*, 2202482.
[19] a) T. Hu, M. S. Molokeev, Z. Xia, Q. Zhang, *J. Mater. Chem. C* **2019**, *7*, 14594; b) T. Yuan, F. Yuan, X. Li, Y. Li, L. Fan, S. Yang, *Chem. Sci.* **2019**, *10*, 9801.
[20] S. He, F. Xu, T. Han, Z. Lu, W. Wang, J. Peng, F. Du, F. Yang, X. Ye, *Chem. Eng. J.* **2020**, *392*, 123657.
[21] S. J. Park, H. K. Yang, B. K. Moon, *Dyes Pigments* **2021**, *186*, 109063.
[22] a) T. Zhang, Y. Wu, X. Ma, *Chem. Eng. J.* **2021**, *412*, 128689; b) Y. Zhu, Y. Guan, Y. Deng, Y. Niu, C. Ren, C. Long, Q. Su, P. Wang, *ACS Appl. Polym. Mater.* **2022**, *4*, 5638.

